Phytomedicine 22 (2015) 1223–1231

Contents lists available at ScienceDirect

Phytomedicine

journal homepage: www.elsevier.com/locate/phymed

Activity of *Artemisia annua* and artemisinin derivatives, in prostate carcinoma

Friedrich-Wilhelm Michaelsen[a,1], Mohamed E.M. Saeed[b], Jörg Schwarzkopf[c], Thomas Efferth[b,*]

[a] *Practice for Naturopathy, 29499 Zernien, Germany*
[b] *Department of Pharmaceutical Biology, Institute of Pharmacy and Biochemistry, Johannes Gutenberg University, Mainz, Germany*
[c] *Clinic for General Medicine, 29456 Hitzacker, Germany*

ARTICLE INFO

Article history:
Received 26 September 2015
Accepted 1 November 2015

Keywords:
Asteraceae
Drug resistance
PSA, Sesquiterpene
Tumor imaging
Tumor marker

ABSTRACT

Background: *Artemisia annua* L, artemisinin and artesunate reveal profound activity not only against malaria, but also against cancer *in vivo* and clinical trials. Longitudinal observations on the efficacy of *A. annua* in patients are, however missing as of yet.
Methods: Clinical diagnosis was performed by imaging techniques (MRT, scintigraphy, SPECT/CT) and blood examinations of standard parameters from clinical chemistry. Immunohistochemistry of formalin-fixed, paraffin-embedded tumor material was performed to determine the expression of several biomarkers (cyclooxygenase-2 (COX2), epidermal growth factor receptor (EGFR), glutathione S-transferase P1 (GSTP1), Ki-67, MYC, oxidized low density lipoprotein (lectin-like) receptor 1 (LOX1), p53, P-glycoprotein, transferrin receptor (TFR, CD71), vascular endothelial growth factor (VEGF), von Willebrand factor (CD31)). The immunohistochemical expression has been compared with the microarray-based mRNA expression of these markers in two prostate carcinoma cell lines (PC-3, DU-145).
Results: A patient with prostate carcinoma (pT3bN1M1, Gleason score 8 (4+4)) presented with a prostate specific antigen (PSA) level >800 μg/l. After short-term treatment with bacalitumide (50 mg/d for 14 days) and long-term oral treatment with *A. annua* capsules (continuously 5 × 50 mg/d), the PSA level dropped down to 0.98 μg/l. MRT, scintigraphy and SPECT/CT verified tumor remission. Seven months later, PSA and ostase levels increased, indicating tumor recurrence and skeletal metastases. Substituting *A. annua* capsules by artesunate injections (2 × 150 mg twice weekly *i.v.*) did not prohibit tumor recurrence. PSA and ostase levels rose to 1245 μg/l and 434 U/l, respectively, and MRT revealed progressive skeletal metastases, indicating that the tumor acquired resistance. The high expression of MYC, TFR, and VEGFC in the patient biopsy corresponded with high expression of these markers in the artemisinin-sensitive PC-3 cells compared to artemisinin-resistant DU-145 cells.
Conclusion: Long-term treatment with *A. annua* capsules combined with short-term bicalitumide treatment resulted in considerable regression of advanced metastasized prostate carcinoma. Controlled clinical trials are required to evaluate the clinical benefit of *A. annua* in prostate cancer.

Introduction

In addition to their antimalarial activity, artemisinin from *Artemisia annua* L. and its derivatives also exert remarkable anticancer effects towards cell lines from a broad variety of tumor types (Efferth et al., 2001; Efferth et al., 2002; Efferth et al., 1996; Efferth et al., 2003) including prostate carcinoma (He et al., 2010; Morrissey et al., 2010; Willoughby et al., 2009). Importantly, artemisinin-type drugs are also active against diverse syngeneic animal tumors (Disbrow et al., 2005; Lai and Singh, 2006; Moore et al., 1995) and human xenograft tumors in nude mice (Dell'Eva et al., 2004; Du et al., 2010; Li et al., 2007; Ma et al., 2011). Artesunate also protects from inflammatory and oxidative tissue injury *in vivo* caused by carcinogens (Ng et al., 2014). Compassionate uses of artemisinins and *Artemisia annua* preparations for cancer therapy of veterinary and human tumors encouraged the performance of several clinical phase I/II trials

Abbreviations: COX2, cyclooxygenase 2; CRP, C-reactive protein; EGFR, epidermal growth factor receptor; GSTP1, glutathione S-transferase P1; LOX1, oxidized low density lipoprotein (lectin-like) receptor 1, MRT, magnetic resonance tomography; PSA, prostate-specific antigen, SPECT, single-photon emission computed tomography; TFR, transferrin receptor (CD71); VEGF, vascular endothelial growth factor.

* Corresponding author. Tel.: +49 6131 3925751; fax: +49 6131 3923752.
E-mail address: efferth@uni-mainz.de (T. Efferth).
[1] deceased

http://dx.doi.org/10.1016/j.phymed.2015.11.001
0944-7113/

(Berger et al., 2005; Breuer and Efferth, 2014; Jansen et al., 2011; Krishna et al., 2015; Krishna S, 2014; Rutteman et al., 2013; Singh, 2002; Zhang et al., 2008). A recent placebo-controlled, randomized and double-blind phase II trial in colorectal carcinoma patients demonstrated that patients taking artesunate tablets in addition to standard surgical therapy had a survival advantage (Krishna et al., 2015).

Despite clinical activity of artemisinins against cancer, longitudinal studies on the efficacy of artemisinin and *Artemisia annua* preparations upon longer application times are missing. In the present report, we describe a patient suffering from progressive prostate carcinoma. He was short-term treated with bicalitumide and long-term treated with *A. annua p.o.* and artesunate *i.v.* Initially, this patient responded remarkably well to *A. annua* capsules, but developed artesunate-resistant bone metastases later on.

Patient and methods

Clinical management

The patient was born November 9th 1934. Medical records have been provided by the patient himself with written consent to scientifically evaluate and publish them (letter dated from January 13th 2015).

Magnetic resonance tomography (MRT) was performed at the Kernspinzentrum Europa-Passage 20095 Hamburg, Germany. The histological appraisal of prostate fine needle biopsies were done at the Asklepios Clinics St. Georg (academic teaching hospital of the University of Hamburg), 20099, Hamburg, Germany. Whole body scintigraphy (after injection of 690 MBq Tc-99m-MDP) and SPECT/CT were done at the Radiological Clinic, Uelzen, Germany. Blood parameters were measured by Dr. von Froreich Bioscientia GmbH, Hamburg, Germany.

Treatment with vitamin C, glutathione (Ridolex, 600 mg), citric acid was done in the clinic of Dr. Jörg Schwarzkopf (Hitzacker, Germany). Treatment with *Artemisia annua* was performed by Dr. Walter Weber (Hamburg, Germany) (Artemisinin, Eura-Nutrador, Landgraaf, Netherlands; 50 mg *Artemisia annua* concentrate (with tricalcium phosphate, microcrystalline cellulose, silicium dioxide and magnesium stearate as adjuvants). Artesunate injections were obtained from Dr. Miller GmbH (Hamburg, Germany; 2 × 150 mg, 2 × weekly).

Immunohistochemistry

For determination of protein expression the UltraVision polymer detection method (kit from Thermo Fisher Scientific GmbH, Dreieich, Germany), method was used as previously described. Formalin-fixed, and paraffin-embedded sections were deparaffinated (2 × 2 min xylol) and rehydrated. For antigen retrieval, sections were submerged in Target Retrieval Solution (Thermo Fisher Scientific) for 20 min at 95–99 °C. Afterwards, slides were allowed to cool down at room temperature and washed in phosphate buffered saline (pH 4) for 10 min. Endogenous peroxidase activity was blocked by immersing the slides in 3% H_2O_2 for 10 min at room temperature. After rinsing for 5 min in PBS, non-specific binding was blocked by Ultra Vision Block (Thermo Scientific) for another 5 min. Slides were incubated in a humidified chamber for 1 h at room temperature with primary antibody: EGFR (RM-2111-S0, dilution 1:50, Thermo Scientific), p53 (M3629, dilution: 1:100, DAKO GmbH, Hamburg, Germany), (RM-2111-S0, dilution 1:50, Thermo Scientific), c-Myc (MS-139-PCL, dilution 1:50, Thermo Scientific), Ki-67 (ab16667, dilution 1:100, Abcam, Cambridge, UK), CD31 (MS-353-S0, dilution 1:50, Thermo Scientific), P-glycoprotein (CD243, AM05632PU-N, dilution 1:200, Acris, Herford, Germany), GSTP1 (AP02100SU-S, Acris), COX2 (AM11127PU-N, dilution 1:100, Acris), LOX1 (HPA050798, dilution 1:300, Sigma), TFR (CD71; MS-1096-S0, dilution 1:50, Thermo Scientific), and VEGF (Ab-7, clone VG-1, which recognized 121,165, and 189 isoformes of VEGF; dilution 1:150, Thermo Scientific). After rinsing for 5 min in PBS, Primary Antibody Amplifier Quanto (Thermo Scientific) was applied for 10 min at room temperature. Slides were washed in PBS for 5 min and then HRP Polymer Quanto (Thermo Scientific) was applied for 10 min, a wash step (5 min) followed. Afterwards, 30 μg/l diaminobenzidine (DAB) Quanto chromogen (Thermo Scientific) was mixed with 1 ml DAB Quanto substrate and applied to the slides for 5 min. After washing in PBS for 5 min, the tissues were counterstained in hemalaun solution (Merck KGaA, Darmstadt, Germany) and rinsed in PBS for 5 min, followed by running tap water (10 min). Tissue sections were dehydrated (2 × 1 min 70% ethanol, 2 × 1 min 96% ethanol, 2 × 1 min 100% ethanol, 2 × 5 min xylol, 1 × 2 min xylol) and embedded using Entellan (Merck).

The immunostained slides were scanned by Panoramic Desk (3D Histotech Pannoramic digital slide scanner, Budapest, Ungary) and interpreted (Quantification of immunostained slides) by panoramic viewer software (NuclearQuant and MembraneQuant, 3D HISTECH) in which positive stained nucleus or membrane were counted in each defined annotated area. Evaluation parameters included number of overall detected objects (nucleus or membrane) in each annotated area, average of positivity and intensity. Nuclear stainings (Ki-67, p53, c-Myc, TUNEL) were quantified using the NuclearQuant software and membrane-bound and cytosolic stainings were quantified by the MembraneQuant software (3D HistoQuant).

Cell lines

PC-3 and DU-145 prostate cancer cell lines are part of the drug screening panel of 60 cell lines of the Developmental Therapeutics Program of the National Cancer Institute (Bethesda, MD, USA). The cytotoxicity of 10 artemisinin-type compounds (artemisinin, artemether, arteether, artesunate, artenimol, arteanuin B, one artesunate derivative, and three artemisinin dimers (chemical structures, see Fig. 4) towards PC-3 and DU-145 cells was measured by the sulforhodamine B assay (Monks et al., 1991). The 50% inhibition concentrations calculated from dose response curves and converted to logarithmic values ($\log_{10}IC_{50}$) have been deposited in the NCI database (http://dtp.nci.nih.gov).

Cluster analyses of microarray data

The mRNA microarray hybridization of the NCI cell lines has been reported and deposited at the NCI website (http://dtp.nci.nih.gov) (Amundson et al., 2008; Scherf et al., 2000). For hierarchical cluster analysis, objects were classified by calculation of distances according to the closeness of between-individual distances by means of hierarchical cluster analysis. All objects were assembled into cluster trees (dendrograms) by the algorithm included into the WINSTAT program (Kalmia Co, MA, U.S.A.). The cluster analyses were run using the WARD method. Previously, cluster models have been validated for gene expression profiling and for approaching molecular pharmacology of cancer (Efferth et al., 1997; Villeneuve and Parissenti, 2004; Zeeberg et al., 2011).

Results

Initial clinical presentation

On January 19th 2014, a 80-year old man presented with abdominal pain, weakness, and fever (39.8 °C) on January 21st 2014, which were due to a prostate carcinoma (3.5 cm diameter) and extended ubiquitary skeletal metastases, but without hepatic metastasis as determined by MRT on January 29th 2014. A suspicious lymph node

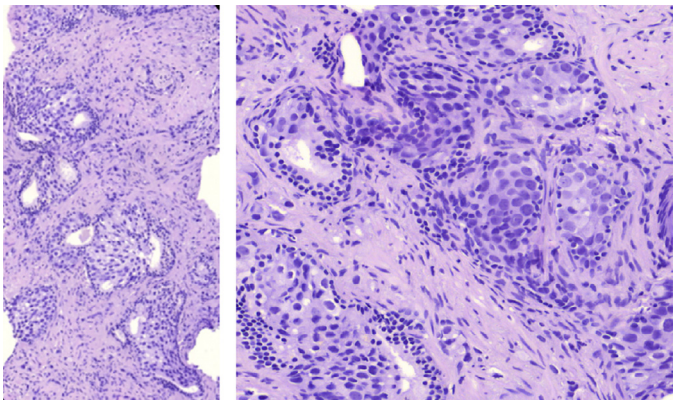

Fig. 1. Histological hematoxilin–eosin staining of the patient tumor. Magnification: (A) ×50; (B) ×200.

(1.4 cm diameter) was found at the left iliacal site. The patient has been treated with weekly vitamin C infusions (2 × 7.5 g), glutathione and citric acid (10 ampulles). Ibuprofen was occasionally taken for pain treatment.

Three weeks later (February 18th 2014), he was hospitalized on an emergency basis because of acute urine failure. A belly-bladder catheter was installed. The PSA level was dramatically elevated to >800 μg/l). The patient obtained 50 mg bicalutamide 1 × 1 for 14 days as hormone ablative therapy and percutaneous cystectomy.

Scintigraphy and SPECT (axial and spiral CT) on March 28th and April 8th 2014 showed extended bone metastasis. Most of the metastases were osteoblastic, but some osteloytic alterations were also visible, especially in the abdominal spine. An intrapulmonal expanding lesion was not observed, but a massive enhancement of the left-sided thyroid lobe. The tumor was staged as pT3bN1M1 and graded with Gleason score 8 (4 + 4). A hematoxilin–eosin staining of the tumor is shown in Fig. 1.

Immunohistochemical detection of tumor markers

The expression of several tumor markers for tumor aggressiveness and progression *e.g.* oncogenes (epidermal growth factor receptor (EGFR), c-MYC) tumor suppressor genes (p53), proliferation markers (transferrin receptor (TFR), Ki-67), drug resistance markers (P-glycoprotein (ABCB1/MDR1), glutathione S-transferase P1 (GSTP1), inflammation markers (cyclooxygenase 2 (COX2), lectin-like oxidized low-density lipoprotein receptor-1 (LOX1) and angiogenic markers (CD31, VEGF) (Figs. 2 and 3). The expression levels of these tumor markers indicate the aggressiveness of the tumor and may also predict responsiveness of the tumor towards artemisinins. Quantification of immunostained slides revealed the highest values for COX2, EGFR, MYC, LOX1, and TFR, whereas P-glycoprotein and p53 expression was lowest. Intermediate to weak expression was found for the other markers investigated (Fig. 4).

Clinical follow-up

Since March 3rd 2014, the patient took *A. annua* capsules (2 × 50 mg twice daily) with a three day break between March 26th–29th 2014. Hemoptysis took place on March 31st 2014. During the treatment break, the amounts of rest urine considerably increased. *A. annua* treatment was then continued with five capsules per day and stopped again on April 10th 2014 because swelling at the left foot ankle. *A. annua* (5 capsules per day) was continued again since April 13th 2014. During this time, the PSA level dramatically dropped down from 580.3 to 0.98 μg/l. Since August 4th 2014, PSA continuously rose again (10.8 μg/l) and reached 1245 μg/l on January 23rd 2015 (Table 1).

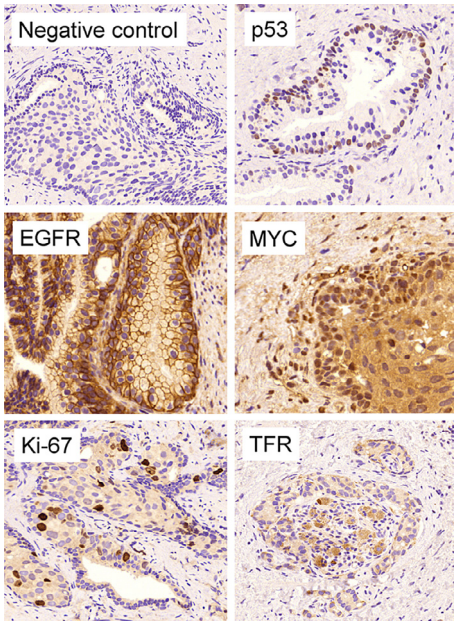

Fig. 2. Immunohistochemical determination of tumor markers in formalin-fixed, paraffin-embedded prostate carcinoma tissue. Immunohistochemical staining of negative control (omitting primary antibody), the tumor suppressor p53 in cell nuclei, oncogenes (membrane-bound EGFR, nuclear and cytosolic c-MYC), proliferation markers (nuclear Ki-67 as well as membrane-bound and cytosolic transferrin receptor (TFR)). For determination of protein expression the UltraVision polymer detection method (kit from Thermo Fisher Scientific GmbH, Dreieich, Germany) was used. Magnification: ×200.

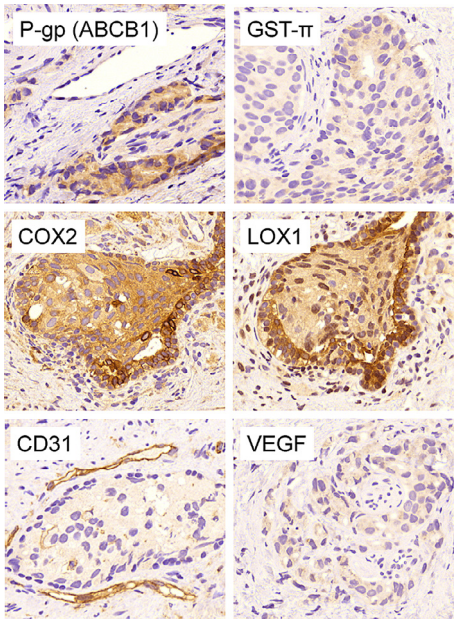

Fig. 3. Immunohistochemical determination of tumor markers (continuation of Fig. 2). Immunohistochemical staining of drug resistance markers (membrane-bound and cytosolic P-glycoprotein (MDR1/ABCB1) as well as cytosolic GST-π), inflammation markers (cytosolic COX2, membrane-bound and cytosolic LOX1) and angiogenic markers (von Willebrand factor (CD31) in blood vessel endothelial cells as well as cytosolic VEGF). Further details see Fig. 2.

Bone-specific alkaline phosphatase (ostase) was elevated at the beginning of the observation period (until May 19th 2014) was in a normal range and increased again since September 29th 2014 reaching a peak level of 434 U/l on January 23rd 2015. This course reflects the tumor and bone metastases regression observed by imaging techniques (MRT, scintigraphy/SPECT). A similar course was visible for CRP (Table 1). Creatinine kinase levels were increased in the majority of blood examinations.

Table 1
Blood count and clinical chemistry.

Parameter	Units	Reference area	January 20th 2014	March 5th 2014	March 25th 2014	April 23rd 2014	April 25th 2014	May 19th 2014	June 5th 2014	August 4th 2014	August 12th2014	September 29th 2014	October 6th 2014	October 14th 2014	November 5th 2014	November 25th 2014	January 6th 2015	January 23rd 2015
Blood count::																		
Leucocytes	count/nL	3,6-10,0	7,9	6,3	3,9	4,8	5,5	4,0	**3,5**	4,1	**3,5**	5,3	4,8	7,0	4,3	5,5	6,5	5,3
Erythrocytes	count/pL	4,3-5,75	4,4	**3,8**	**3,7**	**3,7**	**3,8**	**3,8**	**4,2**	**4,0**	**4,1**	**3,9**	**4,0**	**3,9**	**3,8**	**3,9**	**3,4**	3,1
Hemoglobin	g/dL	12,5-17,2	12,5	**10,7**	**10,5**	**10,3**	**10,9**	**10,8**	**11,8**	**11,5**	**12,4**	**11,6**	**12,0**	**11,3**	**11,2**	**11,4**	**9,6**	8,9
Hematokrit	L/L	0,37-0,49	0,4		**0,3**	**0,3**	**0,3**	**0,3**	0,4	**0,4**	**0,4**	**0,4**	**0,3**	**0,3**	**0,3**	**0,3**	**0,3**	0,3
MCV	fL	80-101	85	87	88	85	86	87	87	90	87	91	87	88	87	86	86	87
MCH	pg	27-34	28,7	28,0	28,3	27,9	28,5	28,5	28,0	29,0	30,0	29,8	30,4	29,0	29,8	29,5	28,7	28,8
MCHC	g/dL	31,5-36	33,9	32,1	32,2	32,9	33,0	32,7	32,2	32,4	34,3	32,7	34,9	33,1	34,3	34,4	33,2	33,0
Thrombocytes	count/nL	140-360	273	274	202	250	240	208	225	202	217	258	214	264	222	240	226	273
Clinical Chemistry:																		
GOT (ASAT)	U/L	<50	34,0	18,0	23,0				21,0	32,0	21,0	20,0	27,0	46,0	21,0	21,0	37,0	**55,0**
GPT (ALAT)	U/L	<50	20,0	14,8	20,0				21,0	21,0	19,0	19,0	20,0	16,0	16,0	13,0	15,0	24,0
gamma-GT	U/L	<60	**72,0**	55,9	45,0			34,0	31,0	24,0	26,0	26,0	26,0	33,0	29,0	39,0	60,0	**74,0**
Bone-specific alkaline phosphatase (ostase)	U/L	40-130	**888**		**978**			**141**	119	76	74	**135**	**146**	**188**	**244**	**350**	**439**	**434**
Lipase	U/L	<60	8,0		20,0				20,0	11,0	13,0	11,0	13,0	8,0	9,0	4,0	7,0	5,0
Amylase	U/L	<110	25,0		48,0				53,0	42,0	47,0	44,0	48,0	40,0	36,0	37,0	39,0	39,0
Creatinin kinase	U/L	<190	119		**410**				**209**	**573**	**264**	**244**	**353**	**220**	**208**	130	125	141
Creatinin kinase-BB	U/L	<25	13,0						14,0	21,0	12,0	13,0	21,0	22,0	18,0	**26,0**	**30,0**	**75,0**
GLDH	U/L	<7,0	7,0		<2				2,5	<2	<2	<2	<2	3,3	2,2	<2	3,5	7,2
Cholesterol	mg/dL	<240	170	189					236	**260**	**253**	239	239	**251**	217	217	209	201
Triglycerides	mg/dL	<150	103	122					83	109	112	133	85	108	88	116	113	105
Glucose	mg/dL	65-100	**119**						**158**	**135**	**187**	**182**	**114**	**215**	**210**	**186**	**105**	**128**
HbA1c	% of Hb	4,8-6,0		**7,4**				**7,3**	**7,1**	7,6	7,8	7,7	7,8	**8,0**	**7,7**	**7,4**	**8,0**	**8,1**
Kreatinin enzymatic	mg/dL	0,72-1,18	1,0					0,8	0,9	0,9	0,9	0,9	0,8	0,9	0,9	0,8	0,8	0,9
Urea	mg/dL	3,5-7,2	4,2	4,9					5,7	5,3	5,6	4,6	4,6	4,6	4,8	4,3	4,5	5,1
CRP	mg/L	<5,0	**254**		**11,3**	6,4	28,5	<5	<5	<5	<5	10,2	6,5	**13,2**	**37,8**	**31,9**	**52,1**	**70,0**
Natrium	mmol/L	135-145	**134**			**132**	**133**	**134**	138	136	135	**131**	135	133	135	**129**	136	137
Potassium	mmol/L	3,5-5,1	**5,8**			**5,5**	4,7	4,9	4,8	4,7	5,1	**8,0**	4,7	4,7	5,0	5,4	4,9	4,7
Calcium	mmol/L	2,2-2,65	**1,9**			**2,0**	**1,9**	2,2	**2,1**	2,3	2,3	2,3	2,2	2,2	2,3	2,4	2,3	2,2
Selen	µg/l	50-120				92	111	99	118									
Vitamin B12	ng/L	>300			836													
Vitamin D	µg/l	30-100				**23,9**	**26,4**	**28,8**		33,4	33,6	26,2	63,6				43,2	39,8
Iron	µmol/L	13-32			13,0	**11,0**	**8,0**	14,0	13,0	15,0	14,0	**12,0**	**10,0**	**8,0**	**11,0**	15,0	**12,0**	**12,0**
Ferritin	µg/l	30-400			334	227	302	243	233	241	325	311	**427**	**792**	**788**	**1239**	**1670**	**>2000**
Transferrin	g/L	2-3,6				2,3	2,2	2,2	2,4	2,4	2,3	2,3	2,3	2,3	**1,8**	2,0		**1,9**
Transferrin saturation	%	16-45						25,3										
total iron binding capacity	µmol/L	48-78						54,7										
Tumor marker:																		
PSA	µg/l	<4	**580**		**27,0**	1,9	1,8	1,0	1,4	**10,1**	**14,9**	**46,2**	**63,6**	**82,3**	**133**	**638**	**1166**	**1245**

bold number: below reference area

bold number in grey box : above reference area

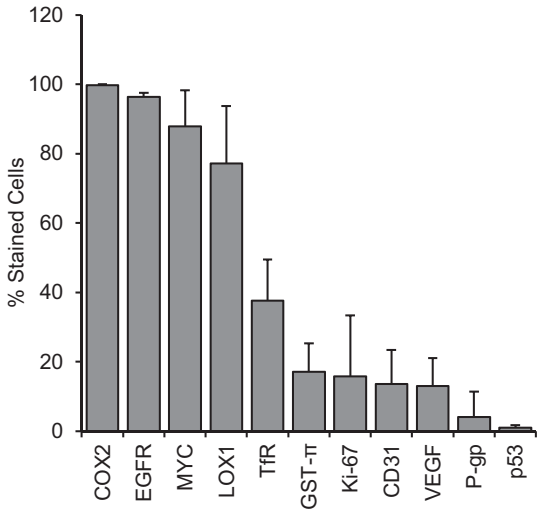

Fig. 4. Quantification of immunohistochemical stainings. The immunostained slides were scanned by Panoramic Desk (3D Histotech Pannoramic digital slide scanner, Budapest, Hungary) and interpreted (Quantification of immunostained slides) by panoramic viewer software (NuclearQuant and MembraneQuant, 3D HISTECH) in which positive stained nucleus or membrane were counted in each defined annotated area. Evaluation parameters included number of overall detected objects (nucleus or membrane) in each annotated area, average of positivity and intensity. Nuclear stainings (Ki-67, p53, MYC) were quantified using the NuclearQuant software and Membrane-bound and cytosolic staining was quantified by the MembraneQuant software (P-glycoprotein, EGFR, GSTP1, COX2. LOX1, CD31, CD71, VEGF).

As a possible side effect, the erythrocyte counts and hemoglobin levels decreased and remained below standard range throughout the entire observation period (Table 1). Liver transaminases (GOT, GPT, γ-GT) and fat metabolism (cholesterol, triglycerides) were obviously not affected by artemisinin. The elevated glucose level was unrelated to artemisinin treatment because of preexisting Diabetes mellitus. Imbalance of iron metabolism (free iron and ferritin) was more imbalanced at late stage tumor progression.

In addition to prostate carcinoma-related symptoms, several lipomas at the inner side of thighs, which had been developed during the past five years, significantly regressed upon artemisinin treatment.

MRT analysis on August 11th 2014 revealed a decrease of the size of the primary tumor in the prostate by 50% as well as considerably decreased skeletal metastases in the pelvis area. Lymphogenic metastasis was not detectable.

Comparable results were found by means of scintigraphy and SPECT (August 28th 2014). Metastases were reduced on spine and pelvis, especially Os sacrum and right proximal femur. However, new lesions appeared in a ventral rib. The existing metastases at the left proximal humerus and ribs at both sides remained unchanged.

The further course went worse as determined by spiral CT on December 8th 2014. Progressive diffuse, mainly osteoblastic metastasis of the entire skeleton was detected with progressive single lytic areas in the abdominal vertebrae channel. There was suspicion on hemangioma in the lumbar vertebrae channel and the prostate was significantly increased. At that time, treatment with *A. annua* capsules was ceased and exchanged by artesunate *i.v.* infusions (2 × 150 mg twice weekly) and continued for the following months with occasional interruptions for not more than one week. MRT showed refractory skeletal metastases in femur, pelvis and lumbar spine as well as significantly increased prostate and three increased lymph nodes. The patient died at April 3rd 2015.

Tumor marker expression and sensitivity towards artemisinin-type compounds in two prostate cancer cell lines

In order to better understand the relevance of the tumor marker expression shown in Figs. 2 and 3, we compared these biomarkers with the sensitivity to a panel of artemisinin derivatives in two prostate cancer cell lines. The $\log_{10}IC_{50}$ values of 10 artemisinin-type compounds (artemisinin, artemether, arteether, artesunate, artenimol, arteanuin B, one artesunate derivative, and three artemisinin dimers, Fig. 6) and the microarray-based expression values of 11 tumor markers (*ABCB1, GSTP1, COX2, LOX1, EGFR, MYC, KI67, TFR, VEGFA, VEGFB, VEGFC)* of PC-3 and DU-145 prostate cancer cells have been deposited in the database of the National Cancer Institute (NCI, USA). The sensitivities of PC-3 and DU-145 cells to these artemisinin-type compounds are illustrated as oncobiogram in Fig. 5. The axes of this net-like representation show the $\log_{10}IC_{50}$ values in a range from 0 to −8 M for each compound. DU-145 cells were more resistant than PC-3 cells to these compounds except to artemether and arteanuin B. Hence, it can be concluded that DU-145 cells reveal a phenotype resembling resistance to most artemisinin-type compounds, whereas PC-3 cells exert artemisinin sensitivity.

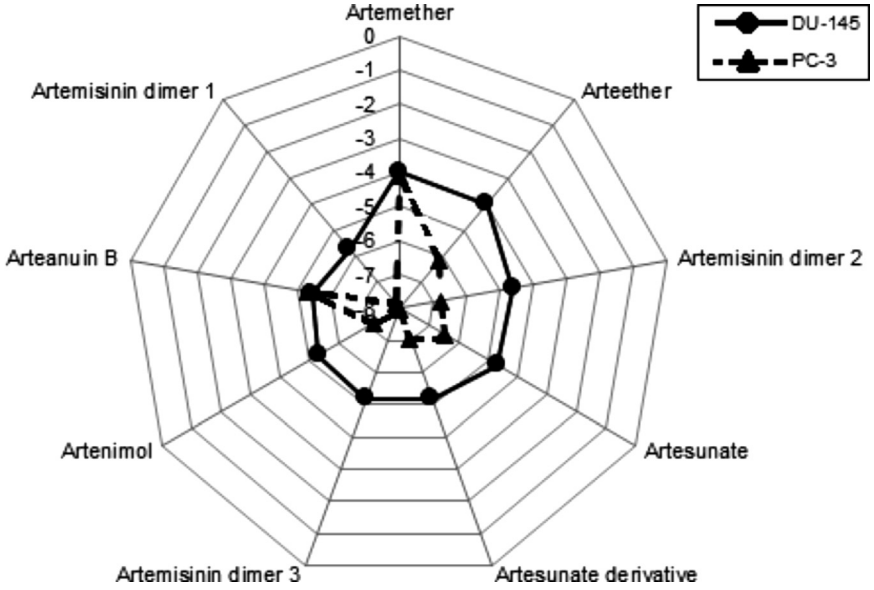

Fig. 5. Resistance profile towards artemisinin derivatives of PC-3 and DU-145 prostate cancer cell lines. The $\log_{10}IC_{50}$ values of sensitive PC-3 and resistant DU-145 cells have been represented as oncobiogram. The chemical structures of these compounds have been recently published (Ooko et al., 2105).

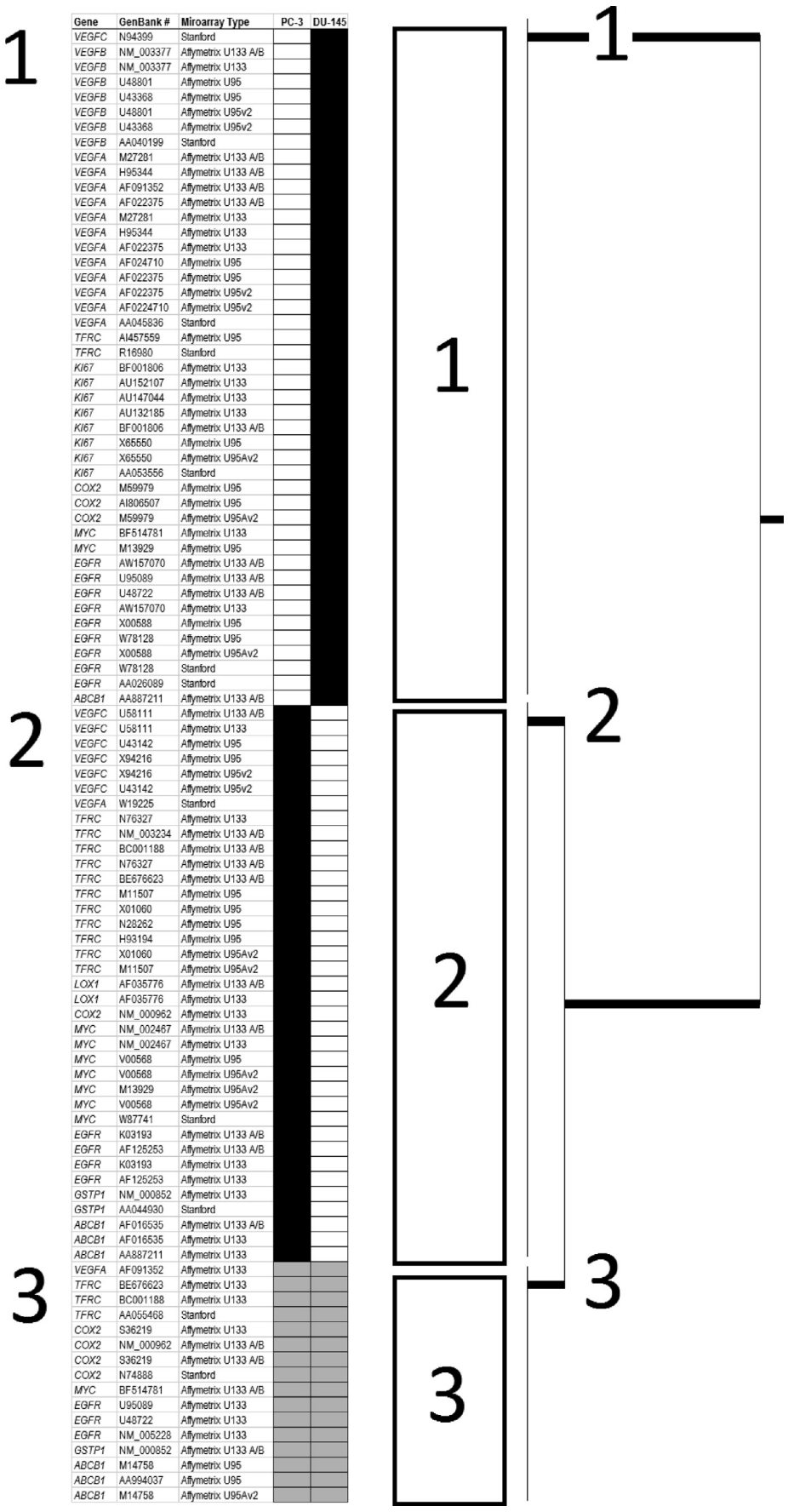

Gene	GenBank #	Miroarray Type	PC-3	DU-145
VEGFC	N94399	Stanford		
VEGFB	NM_003377	Affymetrix U133 A/B		
VEGFB	NM_003377	Affymetrix U133		
VEGFB	U48801	Affymetrix U95		
VEGFB	U43368	Affymetrix U95		
VEGFB	U48801	Affymetrix U95v2		
VEGFB	U43368	Affymetrix U95v2		
VEGFB	AA040199	Stanford		
VEGFA	M27281	Affymetrix U133 A/B		
VEGFA	H95344	Affymetrix U133 A/B		
VEGFA	AF091352	Affymetrix U133 A/B		
VEGFA	AF022375	Affymetrix U133 A/B		
VEGFA	M27281	Affymetrix U133		
VEGFA	H95344	Affymetrix U133		
VEGFA	AF022375	Affymetrix U133		
VEGFA	AF024710	Affymetrix U95		
VEGFA	AF022375	Affymetrix U95		
VEGFA	AF022375	Affymetrix U95v2		
VEGFA	AF0224710	Affymetrix U95v2		
VEGFA	AA045836	Stanford		
TFRC	AI457559	Affymetrix U95		
TFRC	R16980	Stanford		
KI67	BF001806	Affymetrix U133		
KI67	AU152107	Affymetrix U133		
KI67	AU147044	Affymetrix U133		
KI67	AU132185	Affymetrix U133		
KI67	BF001806	Affymetrix U133 A/B		
KI67	X65550	Affymetrix U95		
KI67	X65550	Affymetrix U95Av2		
KI67	AA053556	Stanford		
COX2	M59979	Affymetrix U95		
COX2	AI806507	Affymetrix U95		
COX2	M59979	Affymetrix U95Av2		
MYC	BF514781	Affymetrix U133		
MYC	M13929	Affymetrix U95		
EGFR	AW157070	Affymetrix U133 A/B		
EGFR	U95089	Affymetrix U133 A/B		
EGFR	U48722	Affymetrix U133 A/B		
EGFR	AW157070	Affymetrix U133		
EGFR	X00588	Affymetrix U95		
EGFR	W78128	Affymetrix U95		
EGFR	X00588	Affymetrix U95Av2		
EGFR	W78128	Stanford		
EGFR	AA026089	Stanford		
ABCB1	AA887211	Affymetrix U133 A/B		
VEGFC	U58111	Affymetrix U133 A/B		
VEGFC	U58111	Affymetrix U133		
VEGFC	U43142	Affymetrix U95		
VEGFC	X94216	Affymetrix U95		
VEGFC	X94216	Affymetrix U95v2		
VEGFC	U43142	Affymetrix U95v2		
VEGFA	W19225	Stanford		
TFRC	N76327	Affymetrix U133		
TFRC	NM_003234	Affymetrix U133 A/B		
TFRC	BC001188	Affymetrix U133 A/B		
TFRC	N76327	Affymetrix U133 A/B		
TFRC	BE676623	Affymetrix U133 A/B		
TFRC	M11507	Affymetrix U95		
TFRC	X01060	Affymetrix U95		
TFRC	N28262	Affymetrix U95		
TFRC	H93194	Affymetrix U95		
TFRC	X01060	Affymetrix U95Av2		
TFRC	M11507	Affymetrix U95Av2		
LOX1	AF035776	Affymetrix U133 A/B		
LOX1	AF035776	Affymetrix U133		
COX2	NM_000962	Affymetrix U133		
MYC	NM_002467	Affymetrix U133 A/B		
MYC	NM_002467	Affymetrix U133		
MYC	V00568	Affymetrix U95		
MYC	V00568	Affymetrix U95Av2		
MYC	M13929	Affymetrix U95Av2		
MYC	V00568	Affymetrix U95Av2		
MYC	W87741	Stanford		
EGFR	K03193	Affymetrix U133 A/B		
EGFR	AF125253	Affymetrix U133 A/B		
EGFR	K03193	Affymetrix U133		
EGFR	AF125253	Affymetrix U133		
GSTP1	NM_000852	Affymetrix U133		
GSTP1	AA044930	Stanford		
ABCB1	AF016535	Affymetrix U133 A/B		
ABCB1	AF016535	Affymetrix U133		
ABCB1	AA887211	Affymetrix U133		
VEGFA	AF091352	Affymetrix U133		
TFRC	BE676623	Affymetrix U133		
TFRC	BC001188	Affymetrix U133		
TFRC	AA055468	Stanford		
COX2	S36219	Affymetrix U133		
COX2	NM_000962	Affymetrix U133 A/B		
COX2	S36219	Affymetrix U133 A/B		
COX2	N74888	Stanford		
MYC	BF514781	Affymetrix U133 A/B		
EGFR	U95089	Affymetrix U133		
EGFR	U48722	Affymetrix U133		
EGFR	NM_005228	Affymetrix U133		
GSTP1	NM_000852	Affymetrix U133 A/B		
ABCB1	M14758	Affymetrix U95		
ABCB1	AA994037	Affymetrix U95		
ABCB1	M14758	Affymetrix U95Av2		

Fig. 6. Hierarchical cluster analysis (WARD method) of mRNA expression of selected tumor markers in PC-3 and DU-145 prostate cancer cell lines.

Table 2
Distribution of microarray-based mRNA expression of 98 microarray hybridizations from selected tumor markers in PC-3 and DU-145 prostate cancer cells.

Gene	Cluster 1	Cluster 2	Cluster 3
ABCB1	1	3	3
GSTP1	0	2	1
EGFR	9	4	3
MYC	2	7	1
COX2	3	1	4
LOX1	0	2	0
KI67	8	0	0
TFRC	2	11	3
VEGFA	12	1	1
VEGFB	7	0	0
VEGFC	1	6	0
chi square test: $p = 1.29 \times 10^{-6}$			

Then, we subjected the mRNA expression of the 11 biomarkers to hierarchical cluster analysis. We used the expression values of different DNA clones of each of these biomarkers tested with different microarray platforms (Affymetrix U95, U95v2, U133, U133A/U133B and the Stanford microarray platform), which were represented by a total number of 98 different sets of microarray determinations for the two prostate cancer cell lines.

P53 has not been included into this analysis, because both cell lines carry mutated *TP53* genes and an association between the mutational status and artemisinin sensitivity therefore cannot be observed. The same was true for CD31. Here, no mRNA expression values were available. Instead, the protein expression values have been deposited. CD31 expression was very similar between both cell lines and again, a relationship between protein expression and sensitivity to artemisinins was not observable.

The mRNA expression values were very heterogeneous between different microarray platforms and also between different DNA clones of the same gene. To allow a comparison between the 98 sets of microarray data, we semiquantitatively ranked the expression with numbers (0, 1, 2). If the mRNA expression was more than 20% different between the two prostate cancer cell lines, the lower value was designated with "0" and the higher value with "2". If the mRNA expression was similar between the cell lines, both were coded with "1". These rank numbers were subjected to hierarchical cluster analysis and a dendrogram with three branches (clusters) was yielded (Fig. 6). Cluster 1 contained genes with high expression in the artemisinin-sensitive PC-3 cells and low expression in resistant DU-145 cells, while the expression was *vice versa* in cluster 2. Cluster 3 contained genes with equal expression levels in both cell lines. To prove, whether this cluster formation contains meaningful information we tested the distribution of genes in the different clusters by chi-square test (Table 2). Although the data set as a whole was statistical significant ($p = 1.29 \times 10^{-6}$), not all genes were differentially expressed between the three clusters. The DNA clones for EGFR, KI67, VEGFA and VEGFB showed the highest expression in cluster 1, while. LOX1, MYC, TFRC and VEGFC expression most frequently high in cluster 2. The other genes were more or less equally distributed among the three clusters.

Discussion

The anticancer activity of artemisinin is a matter of ongoing discussion. Recent clinical trials indicate that the artemisinin derivative, artesunate, inhibited cancer growth of colorectal cancer patients in a placebo-controlled, randomized, double-blind clinical phase II pilot study (Jansen et al., 2011; Krishna et al., 2015; Krishna S, 2014). Here, we report on a patient, whose primary tumor in the prostate initially responded astonishing well to *A. annua* capsules *per os*. The patient suffered from an advanced tumor as shown by radiological and immunohistochemical methods. An impressive decrease of the tumor marker PSA and tumor regression as analyzed by imaging techniques (MRT, scintigraphy/SPECT) was observed upon *A. annua* treatment followed by a several months lasting period free of symptoms of the tumor disease.

PSA is an established biomarker for the course of prostate carcinoma, which is routinely used to monitor treatment success (Crawford et al., 2013). Here, the initial decline and subsequent rise of PSA levels upon *A. annua* treatment levels showed that the PSA may also be a useful marker to monitor the efficacy of artemisinin treatment in prostate carcinoma patients.

Interestingly, the inflammation marker CRP also declined upon *A. annua* treatment indicating that tumor-related inflammatory processes have been beneficially influenced by *A. annua.* In the refractory state, CRP rose again. CRP has been described as prognostic factor associated with worse overall survival of prostate cancer patients (Rocha et al., 2014).

Creatinine kinase is a marker for muscle damage, and increased creatinine kinase levels correlate with the risk for myocardial infarction. On the other hand, increased creatinine kinase BB levels can also serve as a tumor marker for various carcinoma types (Arenas et al., 1989) and elevated levels pf the creatinine kinase BB isoenzyme have been observed in poorly differentiated prostate carcinoma (Silverman et al., 1981). The creatinine kinase increase in the late observation phase of the patient may therefore reflect tumor recurrence.

The increased activity of bone-specific alkaline phosphatase (also termed ostase) was in accordance to the osteolytic metastatic lesions of the patient. This enzyme hydrolyzes phosphoric acid esters and is involved in bone destructive processes. Hence, this enzyme can be used as marker to monitor bone metastasis in prostate carcinoma and other tumor types (Cooper et al., 1994).

The anticancer activity of artemisinin and its derivatives has been linked to the iron metabolism (Efferth et al., 2004; Kelter et al., 2007). The cleavage of artemisinin's endoperoxide moiety is facilitated by iron II ions in a Fenton-type reaction (Haynes et al., 2012). Therefore, the blood contents of free iron and organically bound iron in the form of ferritin and transferrin have been measured. The amounts of free iron and ferritin were more imbalanced during late tumor recurrence. Whether this was associated to tumor progression in general or specifically to the development of artemisinin resistance remains unclear.

Cancer chemotherapy is frequently hampered by severe side effects. Artemisinin is known to exert few and tolerable side effects both in malaria and cancer therapy (Efferth and Kaina, 2010; Jansen et al., 2011; Krishna et al., 2015; Krishna S, 2014). The patient of the present case report experiences a decrease in erythrocytes and hemoglobin levels. This is in accordance with preclinical *in vivo* data reporting on toxicity towards reticulocytes as precursor cells of erythrocytes (Clark et al., 2011).

Liver transaminases of the patient were within the normal range. Hence, we do not have reason to speculate on hepatotoxicity induced by *A. annua*. Other side effects known from cancer therapy with artemisinin derivatives (flu-like symptoms, abdominal pain) (Jansen et al., 2011) or from preclinical dose escalation studies in animals (*e.g.* neurotoxicity) (Li and Hickman, 2011) did not appear in this patient. By contrast, *A. annua* treatment was accompanied by an increase of life quality of the patient (good mood, no pain, very active). This was an observation that has also been made in veterinary cancer patients (dogs) that have been treated with an *A. annua* preparation (Dr. Elmar Breuer, Müllheim, personal communication).

The initial dramatic tumor regression was not reached by treatment with *A. annua* alone, but was supported by a short-term treatment with bicalitumide for two weeks. The hormone-ablative bicalitumide has been shown to significantly prolong the survival time of prostate cancer patients, if applied as monotherapy

(Akaza et al., 2009; Kang et al., 2014; Klotz et al., 2014). In baculitamide-based combination regimes, many trials did not show survival advantage as compared to bicalitumide monotherapy (Nakabayashi et al., 2012; Sridhar et al., 2014; Vuky et al., 2012; Wadhwa et al., 2011). Hence, it can be suggested that a combination of artemisinin/artesunate plus bicalitumide may be beneficial.

The transient increase of PSA levels since August 4th 2014 indicated tumor recurrence and beginning of the terminal phase of the disease. At that time, *A. annua* treatment was substituted by artesunate infusions. It is known that *i.v.* application of artemisinin and artesunate leads to longer half-life times and higher peak plasma concentrations than oral application (Batty et al., 1998; Teja-Isavadharm et al., 2001). The expected increased anti-tumor activity and regression of tumor masses did, however, not take place indicating that the tumor acquired resistance to artemisinin and artesunate. Indeed, progressive bone metastases were diagnosed by MRT. While resistance to artemisinins has been observed several times in malaria patients (Mok et al., 2015; Winzeler and Manary, 2014), resistance of cancer cells to this drug is a novel phenomenon. Only two investigations recently reported both inherent and acquired resistance to artemisinin derivatives (Bachmeier et al., 2011; Park et al., 2014). To the best of our knowledge, the present paper represents the first report on clinical artesunate resistance in a cancer patient.

The development of drug resistance has dogged cancer chemotherapy since the very early days back in the 1940s (Rhoads, 1947) and still is a major obstacle today. Therefore, resistance to artemisinin and its derivatives does not come as a surprise. However, novel strategies to prevent or overcome resistance of tumors to artemisinin are urgently needed now to keep this drug active for the sake of future cancer patients.

In this context, it is of interest to predict and to monitor the development of resistance to artemisinins. The immunohistochemical detection of tumor markers has been suggested as strategy to predict, whether or not tumors will respond to cancer chemotherapy (Volm et al., 2004). If successful, this strategy may help to improve treatment outcome in each individual cancer patient. Hence, it is worthwhile to apply this concept also for personalized treatment with artemisinin-type drugs. The determination of tumor markers in artemsinin-sensitive PC-3 and artemisinin-resistant DU-145 prostate carcinoma cells showed that high *TFR, LOX1, MYC,* and *VEGFC* expression was found in sensitive PC-3 cells and high *EGFR, KI67, VEGFA,* and *VEGFB* expression in resistant DU-145 cells. The expression of the other markers did not much vary between the two cell lines. This fits to previously published data. High transferrin receptor expression is associated with enhanced iron uptake, which favors the generation of reactive oxygen species by breaking artemisinin's endoperoxide bridge in a Fenton-type chemical reaction (Efferth et al., 2004; Kelter et al., 2007). MYC has also been described as a factor that is associated sensitivity to artemisinin compounds (Sertel et al., 2010). A possible role of the inflammation marker LOX1 is new and has not been described as of yet. On the other hand, EGFR expression was associated with resistance to artesunate (Efferth et al., 2003; Konkimalla et al., 2009).

Ki-67 is an important marker for tumor proliferation. The correlation of high *Ki-67* mRNA expression in PC-3 cells and low expression in DU-145 fits to immunohistochemical Ki-67 stainings in a clinical pilot study on cervical cancer on the responsiveness towards artenimol (Jansen et al., 2011), but not to recent results in a phase II trial in colorectal rectal carcinoma treated with artesunate (Krishna et al., 2015). Further analyses have to further investigate the role of Ki-67 for treatment with artemisinin-type drugs.

Artemisinin and its derivatives are well-known to inhibit angiogenesis by down-regulation of VEGF (Chen et al., 2004). The influence of VEGF expression on artemisinin responsiveness of tumor cells has not been addressed yet. VEGFA and VEGFC are known as prognostic markers in prostate cancer associated with clinical recurrence and metastasis (Jennbacken et al., 2005; Mori et al., 2010; Yang et al., 2006). Here, we observed that artemisinin-resistant DU-145 prostate cancer cells expressed more VEGFA and VEGFB but less VEGFC than sensitive PC-3 cells. The implications of this result deserve further investigation.

The high expression of MYC, TFR, and VEGFC in the patient biopsy corresponded with high expression of these markers in the artemisinin-sensitive PC-3 cells compared to artemisinin-resistant DU-145 cells.

At later stages, as resistance towards *A. annua* developed, it was not possible to obtain tumor biopsies from primary or metastatic tumor sites to compare changes in tumor marker expression in comparison to the biopsy taken at the beginning of *A. annua* therapy.

In conclusion, in the present case report we describe the profound activity of *A. annua* capsules in a patient with progressive and metastasized prostate carcinoma. The remarkable sensitivity of the tumor towards *A. annua* was followed by the development of resistance. New strategies are needed not only to implement *A. annua* and artemisinin-based therapy to obtain tumor regressions, but also to prevent and overcome tumor resistance to artemisinin. A general problem of chemotherapy is that effective drugs frequently loose therapeutic power by the development of resistance phenomena. This is not true for cancer alone, but also for many infectious diseases, *e.g.* malaria. A pessimist would ask at this point: Why should this not be the same destiny for artemisinin-type drugs as for established drugs alike? An optimist would, however, argue that the early awareness of possible artemisinin responsiveness allows monitoring treatment efficacy.

Conflict of interest

There is no conflict of interest.

Acknowledgment

The technical and secretarial assistance of Mrs. Doris Rohr and Mrs. Ilona Zirbs is gratefully acknowledged.

References

Akaza, H., Hinotsu, S., Usami, M., Arai, Y., Kanetake, H., Naito, S., Hirao, Y., 2009. Combined androgen blockade with bicalutamide for advanced prostate cancer: long-term follow-up of a phase 3, double-blind, randomized study for survival. Cancer 115, 3437–3445.

Amundson, S.A., Do, K.T., Vinikoor, L.C., Lee, R.A., Koch-Paiz, C.A., Ahn, J., Reimers, M., Chen, Y., Scudiero, D.A., Weinstein, J.N., Trent, J.M., Bittner, M.L., Meltzer, P.S., Fornace Jr., A.J., 2008. Integrating global gene expression and radiation survival parameters across the 60 cell lines of the National Cancer Institute Anticancer Drug Screen. Cancer Res. 68, 415–424.

Arenas, J., Diaz, A.E., Alcaide, M.J., Santos, I., Martinez, A., Culebras, J.M., 1989. Serum CK-BB as a tumor marker in patients with carcinoma confirmed histologically. Clin. Chim. Acta 182, 183–193.

Bachmeier, B., Fichtner, I., Killian, P.H., Kronski, E., Pfeffer, U., Efferth, T., 2011. Development of resistance towards artesunate in MDA-MB-231 human breast cancer cells. PLoS One 6, e20550.

Batty, K.T., Le, A.T., Ilett, K.F., Nguyen, P.T., Powell, S.M., Nguyen, C.H., Truong, X.M., Vuong, V.C., Huynh, V.T., Tran, Q.B., Nguyen, V.M., Davis, T.M., 1998. A pharmacokinetic and pharmacodynamic study of artesunate for vivax malaria. Am. J. Trop. Med. Hyg. 59, 823–827.

Berger, T.G., Dieckmann, D., Efferth, T., Schultz, E.S., Funk, J.O., Baur, A., Schuler, G., 2005. Artesunate in the treatment of metastatic uveal melanoma–first experiences. Oncol Rep 14, 1599–1603.

Breuer, E., Efferth, T., 2014. Treatment of Iron-Loaded Veterinary Sarcoma by Artemisia annua. Nat. Prod. Bioprospect. 4, 113–118.

Chen, H.H., Zhou, H.J., Wu, G.D., Lou, X.E., 2004. Inhibitory effects of artesunate on angiogenesis and on expressions of vascular endothelial growth factor and VEGF receptor KDR/flk-1. Pharmacology 71, 1–9.

Clark, R.L., Brannen, K.C., Sanders, J.E., Hoberman, A.M., 2011. Artesunate and artelinic acid: association of embryotoxicity, reticulocytopenia, and delayed stimulation of hematopoiesis in pregnant rats. Birth Defects Res. B Dev. Reprod. Toxicol. 92, 52–68.

Cooper, E.H., Whelan, P., Purves, D., 1994. Bone alkaline phosphatase and prostate-specific antigen in the monitoring of prostate cancer. Prostate 25, 236–242.

Crawford, E.D., Bennett, C.L., Andriole, G.L., Garnick, M.B., Petrylak, D.P., 2013. The utility of prostate-specific antigen in the management of advanced prostate cancer. BJU Int. 112, 548–560.
Dell'Eva, R., Pfeffer, U., Vene, R., Anfosso, L., Forlani, A., Albini, A., Efferth, T., 2004. Inhibition of angiogenesis in vivo and growth of Kaposi's sarcoma xenograft tumors by the anti-malarial artesunate. Biochem. Pharmacol. 68, 2359–2366.
Disbrow, G.L., Baege, A.C., Kierpiec, K.A., Yuan, H., Centeno, J.A., Thibodeaux, C.A., Hartmann, D., Schlegel, R., 2005. Dihydroartemisinin is cytotoxic to papillomavirus-expressing epithelial cells in vitro and in vivo. Cancer Res. 65, 10854–10861.
Du, J.H., Zhang, H.D., Ma, Z.J., Ji, K.M., 2010. Artesunate induces oncosis-like cell death in vitro and has antitumor activity against pancreatic cancer xenografts in vivo. Cancer Chemother. Pharmacol. 65, 895–902.
Efferth, T., Benakis, A., Romero, M.R., Tomicic, M., Rauh, R., Steinbach, D., Hafer, R., Stamminger, T., Oesch, F., Kaina, B., Marschall, M., 2004. Enhancement of cytotoxicity of artemisinins toward cancer cells by ferrous iron. Free Radic. Biol. Med. 37, 998–1009.
Efferth, T., Dunstan, H., Sauerbrey, A., Miyachi, H., Chitambar, C.R., 2001. The anti-malarial artesunate is also active against cancer. Int. J. Oncol. 18, 767–773.
Efferth, T., Fabry, U., Osieka, R., 1997. Apoptosis and resistance to daunorubicin in human leukemic cells. Leukemia 11, 1180–1186.
Efferth, T., Kaina, B., 2010. Toxicity of the antimalarial artemisinin and its dervatives. Crit. Rev. Toxicol. 40, 405–421.
Efferth, T., Olbrich, A., Bauer, R., 2002. mRNA expression profiles for the response of human tumor cell lines to the antimalarial drugs artesunate, arteether, and artemether. Biochem. Pharmacol. 64, 617–623.
Efferth, T., Rücker, G., Falkenberg, M., Manns, D., Olbrich, A., Fabry, U., Osieka, R., 1996. Detection of apoptosis in KG-1a leukemic cells treated with investigational drugs. Arzneimittelforschung 46, 196–200.
Efferth, T., Sauerbrey, A., Olbrich, A., Gebhart, E., Rauch, P., Weber, H.O., Hengstler, J.G., Halatsch, M.E., Volm, M., Tew, K.D., Ross, D.D., Funk, J.O., 2003. Molecular modes of action of artesunate in tumor cell lines. Mol. Pharmacol. 64, 382–394.
Haynes, R.K., Cheu, K.W., Chan, H.W., Wong, H.N., Li, K.Y., Tang, M.M., Chen, M.J., Guo, Z.F., Guo, Z.H., Sinniah, K., Witte, A.B., Coghi, P., Monti, D., 2012. Interactions between artemisinins and other antimalarial drugs in relation to the cofactor model–a unifying proposal for drug action. ChemMedChem 7, 2204–2226.
He, Q., Shi, J., Shen, X.L., An, J., Sun, H., Wang, L., Hu, Y.J., Sun, Q., Fu, L.C., Sheikh, M.S., Huang, Y., 2010. Dihydroartemisinin upregulates death receptor 5 expression and cooperates with TRAIL to induce apoptosis in human prostate cancer cells. Cancer Biol. Ther. 9, 819–824.
Jansen, F.H., Adoubi, I., C.K., J, D.E.C., T, Jansen, N., Tschulakow, A., Efferth, T., 2011. First study of oral Artenimol-R in advanced cervical cancer: clinical benefit, tolerability and tumor markers. Anticancer Res. 31, 4417–4422.
Jennbacken, K., Vallbo, C., Wang, W., Damber, J.E., 2005. Expression of vascular endothelial growth factor C (VEGF-C) and VEGF receptor-3 in human prostate cancer is associated with regional lymph node metastasis. Prostate 65, 110–116.
Kang, Y.J., Kim, K.H., Lee, K.S., 2014. Efficacy of Bicalutamide 150-mg monotherapy compared with combined androgen blockade in patients with locally advanced prostate cancer. Korean J. Urol. 55, 315–320.
Kelter, G., Steinbach, D., Konkimalla, V.B., Tahara, T., Taketani, S., Fiebig, H.H., Efferth, T., 2007. Role of transferrin receptor and the ABC transporters ABCB6 and ABCB7 for resistance and differentiation of tumor cells towards artesunate. PLoS One 2, e798.
Klotz, L., Drachenberg, D., Singal, R., Aprikian, A., Fradet, Y., Kebabdjian, M., Zarenda, M., Chin, J., 2014. An open-label, phase 2 trial of bicalutamide dose escalation from 50 mg to 150 mg in men with CAB and castration resistance. A Can. Urol. Res. Consort. Study. Prostate Cancer Prostatic Dis. 17, 320–324.
Konkimalla, V.B., McCubrey, J.A., Efferth, T., 2009. The role of downstream signaling pathways of the epidermal growth factor receptor for Artesunate's activity in cancer cells. Curr. Cancer Drug Targets 9, 72–80.
Krishna, S., Ganapathi, S., Ster, I.C., Saeed, M.E., Cowan, M., Finlayson, C., Kovacsevics, H., Jansen, H., Kremsner, P.G., Efferth, T., Kumar, D., 2015. A randomised, double blind, placebo-controlled pilot study of oral artesunate therapy for colorectal cancer. EBioMed. 2, 82–90.
Krishna S, G.S., Ster IC, Saeed MEM, Cowan M, Finlayson C, Kovacsevics H, Jansen H, Kremsner PG, Efferth T, Kumar D., 2014. A randomized, double-blind, placebo-controlled pilot study of oral artesunate therapy for colorectal cancer., EBioMedicine
Lai, H., Singh, N.P., 2006. Oral artemisinin prevents and delays the development of 7,12-dimethylbenz[a]anthracene (DMBA)-induced breast cancer in the rat. Cancer Lett. 231, 43–48.
Li, L.N., Zhang, H.D., Yuan, S.J., Tian, Z.Y., Wang, L., Sun, Z.X., 2007. Artesunate attenuates the growth of human colorectal carcinoma and inhibits hyperactive Wnt/beta-catenin pathway. Int. J. Cancer 121, 1360–1365.
Li, Q., Hickman, M., 2011. Toxicokinetic and toxicodynamic (TK/TD) evaluation to determine and predict the neurotoxicity of artemisinins. Toxicology 279, 1–9.
Ma, H., Yao, Q., Zhang, A.M., Lin, S., Wang, X.X., Wu, L., Sun, J.G., Chen, Z.T., 2011. The effects of artesunate on the expression of EGFR and ABCG2 in A549 human lung cancer cells and a xenograft model. Molecules 16, 10556–10569.
Mok, S., Ashley, E.A., Ferreira, P.E., Zhu, L., Lin, Z., Yeo, T., Chotivanich, K., Imwong, M., Pukrittayakamee, S., Dhorda, M., Nguon, C., Lim, P., Amaratunga, C., Suon, S., Hien, T.T., Htut, Y., Faiz, M.A., Onyamboko, M.A., Mayxay, M., Newton, P.N., Tripura, R., Woodrow, C.J., Miotto, O., Kwiatkowski, D.P., Nosten, F., Day, N.P., Preiser, P.R., White, N.J., Dondorp, A.M., Fairhurst, R.M., Bozdech, Z., 2015. Drug resistance. Population transcriptomics of human malaria parasites reveals the mechanism of artemisinin resistance.. Science 347, 431–435.
Monks, A., Scudiero, D., Skehan, P., Shoemaker, R., Paull, K., Vistica, D., Hose, C., Langley, J., Cronise, P., Vaigro-Wolff, A., et al., 1991. Feasibility of a high-flux anticancer drug screen using a diverse panel of cultured human tumor cell lines. J. Natl. Cancer Inst. 83, 757–766.
Moore, J.C., Lai, H., Li, J.R., Ren, R.L., McDougall, J.A., Singh, N.P., Chou, C.K., 1995. Oral administration of dihydroartemisinin and ferrous sulfate retarded implanted fibrosarcoma growth in the rat. Cancer Lett. 98, 83–87.
Mori, R., Dorff, T.B., Xiong, S., Tarabolous, C.J., Ye, W., Groshen, S., Danenberg, K.D., Danenberg, P.V., Pinski, J.K., 2010. The relationship between proangiogenic gene expression levels in prostate cancer and their prognostic value for clinical outcomes. Prostate 70, 1692–1700.
Morrissey, C., Gallis, B., Solazzi, J.W., Kim, B.J., Gulati, R., Vakar-Lopez, F., Goodlett, D.R., Vessella, R.L., Sasaki, T., 2010. Effect of artemisinin derivatives on apoptosis and cell cycle in prostate cancer cells. Anticancer Drugs 21, 423–432.
Nakabayashi, M., Werner, L., Courtney, K.D., Buckle, G., Oh, W.K., Bubley, G.J., Hayes, J.H., Weckstein, D., Elfiky, A., Sims, D.M., Kantoff, P.W., Taplin, M.E., 2012. Phase II trial of RAD001 and bicalutamide for castration-resistant prostate cancer. BJU Int. 110, 1729–1735.
Ng, D.S., Liao, W., Tan, W.S., Chan, T.K., Loh, X.Y., Wong, W.S., 2014. Anti-malarial drug artesunate protects against cigarette smoke-induced lung injury in mice. Phytomedicine 21, 1638–1644.
Ooko, E., Saeed, M.E.M., Kadioglua, O., Sarvi, S., Colak, M., Elmasaoudi, K., Janaha, R., Greten, H.J., Efferth, T., 2015. Artemisinin derivatives induce iron-dependent cell death (ferroptosis) in tumor cells. Phytomedicine 22, 1045–1054.
Park, J., Lai, H.C., Singh, M., Sasaki, T., Singh, N.P., 2014. Development of a dihydroartemisinin-resistant Molt-4 leukemia cell line. Anticancer Res. 34, 2807–2810.
Rhoads, C.P., 1947. Report on a cooperative study of nitrogen mustard (HN2) therapy of neoplastic disease. Trans. Assoc. Am. Phys. 60, 110–117.
Rocha, P., Morgan, C.J., Templeton, A.J., Pond, G.R., Naik, G., Sonpavde, G., 2014. Prognostic impact of C-reactive protein in metastatic prostate cancer: a systematic review and meta-analysis. Oncol. Res. Treat. 37, 772–776.
Rutteman, G.R., Erich, S.A., Mol, J.A., Spee, B., Grinwis, G.C., Fleckenstein, L., London, C.A., Efferth, T., 2013. Safety and efficacy field study of artesunate for dogs with non-resectable tumours. Anticancer Res. 33, 1819–1827.
Scherf, U., Ross, D.T., Waltham, M., Smith, L.H., Lee, J.K., Tanabe, L., Kohn, K.W., Reinhold, W.C., Myers, T.G., Andrews, D.T., Scudiero, D.A., Eisen, M.B., Sausville, E.A., Pommier, Y., Botstein, D., Brown, P.O., Weinstein, J.N., 2000. A gene expression database for the molecular pharmacology of cancer. Nat. Genet. 24, 236–244.
Sertel, S., Eichhorn, T., Simon, C.H., Plinkert, P.K., Johnson, S.W., Efferth, T., 2010. Pharmacogenomic identification of c-Myc/Max-regulated genes associated with cytotoxicity of artesunate towards human colon, ovarian and lung cancer cell lines. Molecules 15, 2886–2910.
Silverman, L.M., Chapman, J.F., Jones, M.E., Dermer, G.B., Pullano, T., Tokes, Z.A., 1981. Creatine kinase BB and other markers of prostatic carcinoma. Prostate 2, 109–119.
Singh, N.P., Verma, K.B., 2002. Case report of a laryngeal squamous cell carcinoma treated with artesunate. Arch. Oncol 10, 279–280.
Sridhar, S.S., Joshua, A.M., Gregg, R., Booth, C.M., Murray, N., Golubovic, J., Wang, L., Harris, P., Chi, K.N., 2015. A phase II study of GW786034 (Pazopanib) with or without bicalutamide in patients with castration-resistant prostate cancerClin. Clin. Genitourin Cancer. 13, 124–129.
Teja-Isavadharm, P., Watt, G., Eamsila, C., Jongsakul, K., Li, Q., Keeratithakul, G., Sirisopana, N., Luesutthiviboon, L., Brewer, T.G., Kyle, D.E., 2001. Comparative pharmacokinetics and effect kinetics of orally administered artesunate in healthy volunteers and patients with uncomplicated falciparum malaria. Am. J. Trop. Med. Hyg. 65, 717–721.
Villeneuve, D.J., Parissenti, A.M., 2004. The use of DNA microarrays to investigate the pharmacogenomics of drug response in living systems. Curr. Top. Med. Chem. 4, 1329–1345.
Volm, M., Koomägi, R., Efferth, T., 2004. Prediction of drug sensitivity and resistance of cancer by protein expression profiling. Cancer Genom. Proteom. 1, 157–166.
Vuky, J., Pham, H.T., Warren, S., Douglass, E., Badiozamani, K., Madsen, B., Hsi, A., Song, G., 2012. Phase II study of long-term androgen suppression with bevacizumab and intensity-modulated radiation therapy (IMRT) in high-risk prostate cancer. Int. J. Radiat. Oncol. Biol. Phys 82, e609–e615.
Wadhwa, V.K., Weston, R., Parr, N.J., 2011. Bicalutamide monotherapy preserves bone mineral density, muscle strength and has significant health-related quality of life benefits for osteoporotic men with prostate cancer. BJU Int. 107, 1923–1929.
Willoughby Sr, J.A., Sundar, S.N., Cheung, M., Tin, A.S., Modiano, J., Firestone, G.L., 2009. Artemisinin blocks prostate cancer growth and cell cycle progression by disrupting Sp1 interactions with the cyclin-dependent kinase-4 (CDK4) promoter and inhibiting CDK4 gene expression. J. Biol. Chem. 284, 2203–2213.
Winzeler, E.A., Manary, M.J., 2014. Drug resistance genomics of the antimalarial drug artemisinin. Genome Biol. 15, 544.
Yang, J., Wu, H.F., Qian, L.X., Zhang, W., Hua, L.X., Yu, M.L., Wang, Z., Xu, Z.Q., Sui, Y.G., Wang, X.R., 2006. Increased expressions of vascular endothelial growth factor (VEGF), VEGF-C and VEGF receptor-3 in prostate cancer tissue are associated with tumor progression. Asian J. Androl. 8, 169–175.
Zeeberg, B.R., Liu, H., Kahn, A.B., Ehler, M., Rajapakse, V.N., Bonner, R.F., Brown, J.D., Brooks, B.P., Larionov, V.L., Reinhold, W., Weinstein, J.N., Pommier, Y.G., 2011. RedundancyMiner: De-replication of redundant GO categories in microarray and proteomics analysis. BMC Bioinf. 12, 52.
Zhang, Z.Y., Yu, S.Q., Miao, L.Y., Huang, X.Y., Zhang, X.P., Zhu, Y.P., Xia, X.H., Li, D.Q., 2008. [Artesunate combined with vinorelbine plus cisplatin in treatment of advanced non-small cell lung cancer: a randomized controlled trial]. Zhong Xi Yi Jie He Xue Bao 6, 134–138.